

Minibands of magnetoplasmons in semiconductor superlattices in a perpendicular external magnetic field

G. Martínez, J. H. Jacobo-Escobar, Pedro H. Hernández, and Gregorio H. Coccoletzi
Instituto de Física, Universidad Autónoma de Puebla, Apartado Postal J-48, Puebla 72570, Mexico

(Received 27 July 1998; revised manuscript received 25 November 1998)

Studies are performed on the minibands and the optical response of magnetoplasmons in periodic stratified structures of highly doped semiconductors accounting for an external magnetic \mathbf{B}_0 field in the perpendicular configuration. Incident light of p polarization is considered to calculate the reflectivities R_{pp} of p polarization and R_{ps} of the conversion from p to s polarization, with the results being interpreted as resonances of Fabry-Perot of the waves in the layers and the allowed minibands and forbidden minigaps of bulk magnetoplasmons in the superlattices. The structures shift to lower frequencies, and at the same time the minigaps enlarge as the strength of the \mathbf{B}_0 field decreases. Variations of the structural parameters and the magnetic field permit us to monitor the minibands and minigaps of mode propagation in the superlattices. [S0163-1829(99)02516-3]

I. INTRODUCTION

Optical properties of multilayer systems have attracted the attention of many works in the past few years since they exhibit interesting features useful for technological applications. In particular, literature has focused on the miniband structures of periodic superlattices and the optical reflectance of electromagnetic (EM) waves incident on semi-infinite superlattices of two different materials.¹⁻⁴ Alternatively, the dispersion relations of surface as well as bulk modes have also been studied.⁵ Two different transfer-matrix approaches have been developed, with the dimensions of the matrices being $N \times N$, and N being the number of waves traveling in a layer. One method constructs the EM fields as a superposition of propagating waves and then uses the boundary conditions on the EM fields at the interfaces of adjacent layers to write equations in terms of the amplitudes and then construct the matrices. The resulting matrices, in general, contain information of both layers.⁵ In the alternative theory,¹⁻⁴ the EM fields are constructed in the same way, and a relation is obtained for the fields at the layer surfaces in terms of the transfer matrix, with this matrix characterizing the single layer. The resulting equations are then used in the boundary conditions to obtain the transfer matrix of multilayer systems as a simple matrix multiplication. In this paper, we follow this latter approach to study the collective excitations of the magnetoplasma and the optical reflectivity of the p -polarized light incident on the truncated superlattice.

Studies of magnetoplasma polaritons have been carried out at interfaces of a semiconductor and a metallic screen accounting for external magnetic fields \mathbf{B}_0 both in the Voigt⁶ and Faraday⁷ configurations. Results of the dispersion relations exhibit propagation windows for the Voigt geometry and a mode that terminates at the cyclotron frequency for the Faraday arrangement. Surface magnetoplasma modes^{8,9} of films have also been reported to propagate: two in the Faraday geometry; and surface, bulk, hybrid surface-bulk, and "complex" modes in the perpendicular configuration. Recent literature deals with the collective excitations in truncated semiconductor¹⁰ and metallic¹¹ superlattices in a trans-

verse magnetic field \mathbf{B}_0 . Dispersion relations were discussed in terms of magnetic-field strength to exhibit the miniband structure of the bulk modes and surface modes for the truncated superlattices. However, to our knowledge, no attention has been given to the optical response for the truncated heterostructure and dispersion relations of the collective normal modes on the periodic artificial media in terms of the Bloch wave vector.¹²

Nonlocal theoretical investigations on the optical response of bimetallic superlattices including plasma mode excitations have been reported. A method has been developed to calculate the p -polarized optical reflectance R_{pp} using the transfer-matrix approach.¹² This method is suitable for our problem at hand; furthermore, we outline that procedure for calculating R_{pp} . The first step is to calculate the transfer matrix of a single film, then use the boundary conditions to obtain the corresponding matrix of a period and invoke Bloch's theorem to calculate the wave vector p of the normal-mode dispersion relations. Finally, a p -polarized wave incident on the truncated binary metallic superlattice can excite two outgoing normal modes, additional to the reflected one. The two transmitted waves are characterized by $Q = n[\omega/c]\sin\theta$ and $\text{Im}(p) > 0$, where n is the index of refraction of the left half-space in contact with the superlattice, with θ being the angle of incidence. Once the transmitted fields are written in terms of the two propagating modes, the boundary conditions are applied to calculate the transmitted amplitudes and thus the optical reflectance.¹²

The paper is presented as follows. In Sec. II we describe the 4×4 transfer-matrix approach, then the dispersion relations of the collective normal magnetoplasma modes and the optical response for the incident p -polarized light, accounting for a \mathbf{B}_0 field along the superlattice axis. Analytic calculations are also shown for the reflectivities R_{pp} of light with p polarization and R_{ps} of the conversion from p to s polarization. Results, discussions, and conclusions are given in Sec. III.

II. FORMALISM

The heterostructure under study is depicted in Fig. 1, z being the growth axis and the xy plane parallel to the inter-

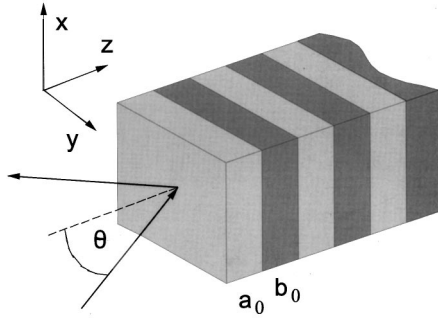


FIG. 1. Schematic representation of the binary semiconductor superlattice. We indicate the coordinate system and layer thicknesses a_0 and b_0 .

faces of the superlattices. The magnetic field \mathbf{B}_0 is along the growth axis; that is, it is considered the perpendicular configuration. Since we are concerned with a local theory, the dielectric-response tensors of the layers are only frequency and magnetic-field dependent, $\tilde{\epsilon}_a$ for layer a and $\tilde{\epsilon}_b$ for layer b , and their thicknesses a_0 and b_0 , respectively. Maxwell's wave equation in a layer can be written as

$$\nabla \times (\nabla \times \mathbf{E}) - q_0^2 \tilde{\epsilon} \cdot \mathbf{E} = 0, \quad (1)$$

where $q_0 = \omega/c$ is the vacuum wave vector. We consider the following nonzero elements of the dielectric tensor in each medium:

$$\epsilon_{xx} = \epsilon_L [1 - \omega_p^2 / (\omega^2 - \omega_c^2)], \quad (2)$$

$$\epsilon_{xy} = -\epsilon_{yx} = i \epsilon_L [\omega_c \omega_p^2 / \omega (\omega^2 - \omega_c^2)], \quad (3)$$

$$\epsilon_{zz} = \epsilon_L [1 - \omega_p^2 / \omega^2], \quad (4)$$

where ϵ_L , ω_p , and ω_c are the background dielectric constant, plasma frequency, and cyclotron frequency, respectively. The dispersion relations obtained from Eq. (1) can be written⁶ as $-q_z^2 = \alpha_{1,2}^2$, with

$$\alpha_{1,2}^2 = \frac{1}{2\epsilon_{zz}} \{ (\epsilon_{xx} + \epsilon_{zz}) Q^2 - 2q_0^2 \epsilon_{xx} \epsilon_{zz} \pm [(\epsilon_{xx} - \epsilon_{zz})^2 Q^4 + 4(Q^2 - q_0^2 \epsilon_{zz}) q_0^2 \epsilon_{xy}^2 \epsilon_{zz}]^{1/2} \}. \quad (5)$$

The electric field has the form

$$\mathbf{E}(\mathbf{r}, t) = \mathbf{E}(\mathbf{z}) e^{i(Qy - \omega t)}, \quad (6)$$

with

$$\mathbf{E}(\mathbf{z}) = \mathbf{E}_1^+ e^{\alpha_1 z} + \mathbf{E}_1^- e^{-\alpha_1 z} + \mathbf{E}_2^+ e^{\alpha_2 z} + \mathbf{E}_2^- e^{-\alpha_2 z}, \quad (7)$$

and the magnetic field is obtained from one of the Maxwell equations, namely, $\nabla \times \mathbf{E} = i[\omega/c] \mathbf{H}$. Following a familiar procedure,^{1-4,12} we write a matrix equation,

$$\begin{pmatrix} \mathbf{E} \\ \mathbf{H} \end{pmatrix}_z = \mathbf{G} \begin{pmatrix} \mathbf{A}_1 \\ \mathbf{A}_2 \end{pmatrix}_z, \quad (8)$$

$$\mathbf{G} = \begin{pmatrix} 1 & 1 & 1 & 1 \\ \gamma_1 & \gamma_1 & \gamma_2 & \gamma_2 \\ -i \frac{\alpha_1}{q_0} & i \frac{\alpha_1}{q_0} & -i \frac{\alpha_2}{q_0} & i \frac{\alpha_2}{q_0} \\ -i \beta_1 \frac{\alpha_1}{q_0} & i \beta_1 \frac{\alpha_1}{q_0} & -i \beta_2 \frac{\alpha_2}{q_0} & i \beta_2 \frac{\alpha_2}{q_0} \end{pmatrix}, \quad (9)$$

where $\gamma_j = -[\epsilon_{xx} q_0^2 - q_{zj}^2 - Q^2] / \epsilon_{xy} q_0^2$ and $\beta_j = [\epsilon_{xx} q_0^2 - q_{zj}^2 - Q^2] \epsilon_{zz} / [\epsilon_{zz} q_0^2 - Q^2] \epsilon_{xy}$, with $j = 1, 2$. We now write a relationship between the fields at two different points z and z' in a layer,

$$\begin{pmatrix} \mathbf{A}_1 \\ \mathbf{A}_2 \end{pmatrix}_z = \mathbf{T}(z - z') \begin{pmatrix} \mathbf{A}_1 \\ \mathbf{A}_2 \end{pmatrix}_{z'}, \quad (10)$$

where $\mathbf{T}(z) = \text{diag}[e^{\alpha_1 z}, e^{-\alpha_1 z}, e^{\alpha_2 z}, e^{-\alpha_2 z}]$ is a diagonal matrix. Finally, using Eqs. (8) and (10) one finds a relationship between the fields evaluated at the film surfaces. This may take the form

$$\begin{pmatrix} \mathbf{E} \\ \mathbf{H} \end{pmatrix}_{z^r} = \mathbf{M}_1 \begin{pmatrix} \mathbf{E} \\ \mathbf{H} \end{pmatrix}_{z^l}, \quad (11)$$

where z^r and z^l stand for the right and left surfaces, respectively, and \mathbf{M}_1 is a 4×4 transfer matrix of a layer with thickness d_1 ,

$$\mathbf{M}_1 = \mathbf{G}_1 \mathbf{T}(d_1) \mathbf{G}_1^{-1}, \quad (12)$$

with the elements having the form

$$M_{11} = [\gamma_2 c_1 - \gamma_1 c_2] / \Delta_2, \quad M_{12} = [-c_1 + c_2] / \Delta_2, \quad (13)$$

$$M_{13} = i q_0 [\beta_2 s_1 / \alpha_1 - \beta_1 s_2 / \alpha_2] / \Delta_1, \quad (14)$$

$$M_{14} = i q_0 [-s_1 / \alpha_1 + s_2 / \alpha_2] / \Delta_1, \quad (15)$$

$$M_{21} = [c_1 - c_2] \gamma_1 \gamma_2 / \Delta_2, \quad M_{22} = [-\gamma_1 c_1 + \gamma_2 c_2] / \Delta_2, \quad (16)$$

$$M_{23} = [\beta_2 \gamma_1 s_1 / \alpha_1 - \beta_1 \gamma_2 s_2 / \alpha_2] i q_0 / \Delta_1, \quad (17)$$

$$M_{24} = [-\gamma_1 s_1 / \alpha_1 + \gamma_2 s_2 / \alpha_2] i q_0 / \Delta_1, \quad (18)$$

$$M_{31} = [-\alpha_1 \gamma_2 s_1 + \alpha_2 \gamma_1 s_2] i / [q_0 \Delta_2], \quad (19)$$

$$M_{32} = i [\alpha_1 s_1 - \alpha_2 s_2] / [q_0 \Delta_2], \quad (20)$$

$$M_{33} = [\beta_2 c_1 - \beta_1 c_2] / \Delta_1, \quad M_{34} = [-c_1 + c_2] / \Delta_1, \quad (21)$$

$$M_{41} = i [-\beta_1 \alpha_1 \gamma_2 s_1 + \beta_2 \alpha_2 \gamma_1 s_2] / [q_0 \Delta_2], \quad (22)$$

$$M_{42} = i [\beta_1 \alpha_1 s_1 - \beta_2 \alpha_2 s_2] / [q_0 \Delta_2], \quad (23)$$

$$M_{43} = \beta_1 \beta_2 [c_1 - c_2] / \Delta_1, \quad M_{44} = [-\beta_1 c_1 + \beta_2 c_2] / \Delta_1, \quad (24)$$

where $c_i = \cosh(\alpha_i d)$, $s_i = \sinh(\alpha_i d)$ with $i = 1, 2$, and

$$\Delta_1 = \beta_2 - \beta_1, \quad \Delta_2 = \gamma_2 - \gamma_1. \quad (25)$$

Assuming that p -polarized light is incident on the semi-infinite superlattice, the electric-field components for $z < 0$ have the form

$$E_y(z) = E_i^p e^{iq_{zv}z} - E_r^p e^{-iq_{zv}z}, \quad E_x(z) = E_r^s e^{-iq_{zv}z}. \quad (26)$$

To obtain the reflectivity $R_{pp} = |E_r^p|^2$, we use the corresponding formula in terms of the surface impedance $Z_p(0)$, written as¹²

$$R_{pp} = \left| \frac{Z_p(0) - Z_v}{Z_p(0) + Z_v} \right|^2, \quad (27)$$

where $Z_v = \cos(\theta)$ and θ is the angle of incidence. We outline how to obtain $Z_p(0)$ and the reflectivity $R_{ps} = |E_r^s|^2$ of the conversion from p to s polarization for the systems under study.

Although the incident light is with p polarization, inside the semiconducting layers, waves have no definite polarization. As illustrated above, the transfer matrix of an isolated semiconducting layer in the presence of an external magnetic field \mathbf{B}_0 is of dimension 4×4 ; furthermore, the corresponding matrix of a two layer system is also 4×4 and is constructed using the boundary conditions at the interface. The result may be written as $\mathbf{M} = \mathbf{M}_2 \mathbf{M}_1$, where the subindices 1 and 2 label layers 1 and 2, respectively. If we consider periodic structures with periods $d = a_0 + b_0$ of two layers and invoke Bloch's theorem, we may write

$$[\mathbf{M} - 1 e^{ipd}] \begin{bmatrix} \mathbf{E} \\ \mathbf{H} \end{bmatrix}_z = 0, \quad (28)$$

where p is again the one-dimensional Bloch wave vector. From this equation one obtains the normal-mode dispersion relation by solving the 4×4 determinant. Results should give four values of p with two of them representing modes traveling to the right and the other two to the left.²

To calculate the surface impedance $Z_p(0)$ of the truncated superlattice, we assume that the surface of the superlattice is at $z=0$. A wave encountering the surface may excite two outgoing (transmitted) normal modes in addition to the reflected wave with p polarization and the conversion from p to s polarization. The transmitted waves are characterized by the wave-vector components Q for the parallel and p for the perpendicular directions to superlattice interfaces, with $\text{Im}(p) > 0$ for the two physical solutions, while the other two possible modes with $\text{Im}(p) < 0$ cannot be normalized in a semi-infinite system, and furthermore their amplitudes must be zero. The transmitted fields at the surface of the superlattice can be written in terms of the eigenvectors of the allowed modes as

$$V(0^+) = \begin{pmatrix} E_x \\ E_y \\ H_y \\ H_x \end{pmatrix}_{0^+} = t_1 \begin{pmatrix} E_x \\ E_y \\ H_y \\ H_x \end{pmatrix}_{0^+}^{(1)} + t_2 \begin{pmatrix} E_x \\ E_y \\ H_y \\ H_x \end{pmatrix}_{0^+}^{(2)}, \quad (29)$$

where t_1 and t_2 are the two undetermined amplitudes, 0^+ stands for the right-hand side of the surface, and the upper indices 1 and 2 label the two modes. At this step, we invoke Maxwell's boundary conditions to obtain t_1 , t_2 , and r , with r

the reflected coefficient. The conditions are the continuity of the tangential components of the electric \mathbf{E} and magnetic \mathbf{H} fields. At $z=0^+$ one may write

$$E_x(0^+) = t_1 E_x^{(1)}(0^+) + t_2 E_x^{(2)}(0^+), \quad (30)$$

$$E_y(0^+) = t_1 E_y^{(1)}(0^+) + t_2 E_y^{(2)}(0^+), \quad (31)$$

$$H_y(0^+) = t_1 H_y^{(1)}(0^+) + t_2 H_y^{(2)}(0^+), \quad (32)$$

$$H_x(0^+) = t_1 H_x^{(1)}(0^+) + t_2 H_x^{(2)}(0^+). \quad (33)$$

Using these results in the surface impedance definition, we obtain

$$Z(0^+) = \frac{E_y(0^+)}{H_x(0^+)} = \frac{\frac{t_1}{t_2} E_y^{(1)}(0^+) + E_y^{(2)}(0^+)}{\frac{t_1}{t_2} H_x^{(1)}(0^+) + H_x^{(2)}(0^+)} \quad (34)$$

and

$$\frac{t_1}{t_2} = \frac{Z_s H_y^{(2)}(0^+) - E_x^{(2)}(0^+)}{E_x^{(1)}(0^+) - Z_s H_y^{(1)}(0^+)}, \quad (35)$$

where $Z_s = q_{zv}/q_0$. Finally, once the amplitudes E_r^p , t_1 , and t_2 are known, E_r^s may be calculated. To obtain the properties for superlattices of alternating a nonisotropic semiconductor and an isotropic insulator, we set $\omega_{p2} = 0$ and use all the results for the binary semiconductor superlattice.

III. RESULTS AND DISCUSSION

Numerical calculations are presented for semiconductor superlattices, considering a \mathbf{B}_0 field applied along the growth axis of the superlattice, perpendicular configuration. The parameters used for the actual calculations are normalized with respect to the plasma frequency of the denser medium; that is, we take $\omega_{p1} = 1$, $\omega_{p2} = 0.25\omega_{p1}$, $\epsilon_{i1} = 13.13$, and $\epsilon_{i2} = 5.02$. To investigate the magnetoplasmon optical properties in the infinite superlattices, we diagonalize numerically the 4×4 transfer matrix to obtain Bloch's wave vector p . Then the reflectivity R_{pp} for p -polarized light as well as the conversion R_{ps} from p to s polarization are calculated for the semi-infinite array. For the optical response we chose solutions that represent physical situations; that is, we considered cases where the imaginary parts of p_i ($i=1,2$) are positive or zero and the real parts as positive. Under these choices, collective excitations may propagate or decay exponentially away from the surface into the volume.

First, we discuss the normal-mode dispersion relation of a superlattice made up of alternating layers of a semiconductor of thickness a_0 and an insulator of thickness b_0 . As the insulator we considered vacuum, therefore we took $\epsilon_i = 1$. In Fig. 2, we display ω vs pd for $\epsilon_i = \epsilon_{i1} = 13.13$, $\omega_p = \omega_{p1}$, $a_0 = b_0 = 0.5c/\omega_p$, and two different cyclotron frequencies $\omega_c = 0.35\omega_p$ and $\omega_c = 0.10\omega_p$. For each wave we considered $Q = (\omega/c)\sin\theta$ of the parallel wave vector, so that the dispersion relations correspond to those modes that may couple the incident light from vacuum at an angle $\theta = 30^\circ$. The left panel shows the real part and the right panel the imaginary

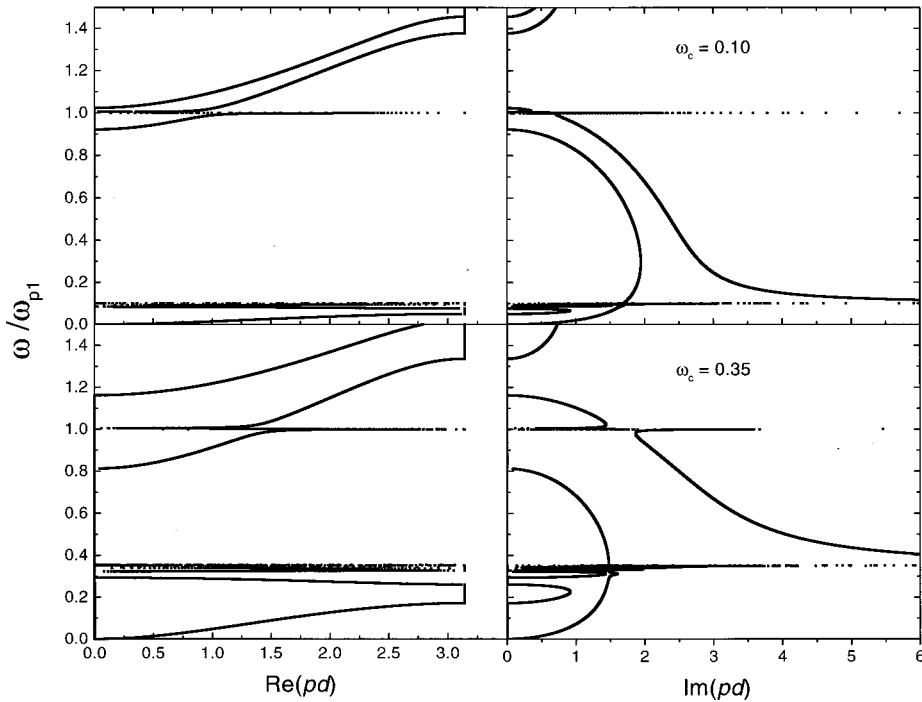


FIG. 2. Real (upper panels) and imaginary (lower panels) parts of p_1 and p_2 of the collective normal-mode dispersion relations as functions of the applied magnetic field, $\omega_c/\omega_p=0.1, 0.35$ for a parallel component of the wave vector $Q=(\omega/c)\sin 30^\circ$ and $a_0=b_0=0.5c/\omega_{p1}$.

part of pd . The minima of the real part are consequences of the Fabry-Perot resonances in the semiconductor layers, as discussed below, with the structure appearing in the frequency region $\omega_c < \omega < \omega_p$. As the strength of \mathbf{B}_0 decreases, the structure shifts to lower frequencies.

To understand the features of Fig. 2, we describe the dispersion relation of the transverse modes that propagate in each semiconductor layer of the superlattice. For that, let us consider a single semiconductor crystal, with the wave vectors α_i ($i=1,2$) as plotted in Fig. 3. Focusing the attention on either upper or lower panels, it is apparent that at ω

$< \omega_c$, of those two transverse waves in the semiconductor layer, one is a propagating mode but the other is not, then we have a pseudosurface (PS) mode region. Above ω_c , a surface mode (SP) regime is obtained, which eventually transforms into a PS mode domain, with this taking place below ω_p . Finally, at frequencies above the plasma frequency, a bulk polariton (BP) mode region is accounted.

The feature exhibited by the real parts of p_1 and p_2 are in close correspondence to that presented by the reflectivity; that is, whenever the real parts of p_1 and p_2 have finite values, the reflectance also takes some finite value. More-

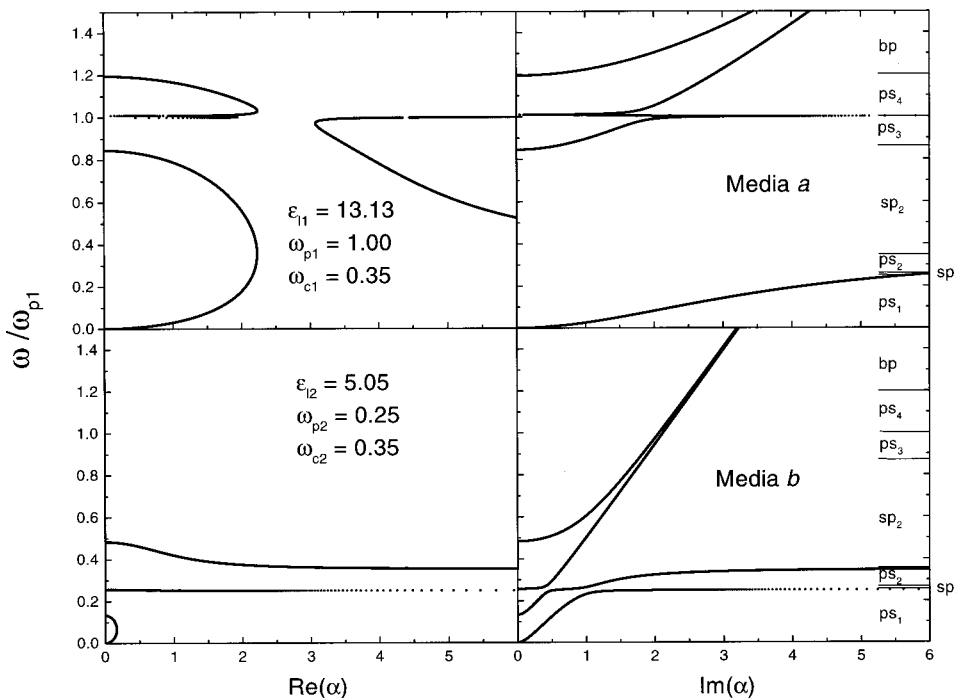


FIG. 3. Real (left panel) and imaginary (right panel) parts of the dispersion relations $\omega = \omega(\alpha_1, \alpha_2)$ for the parameters of Fig. 2. ps_i , sp_i , and bp label the pseudosurface, surface, and bulk polariton frequency regions.

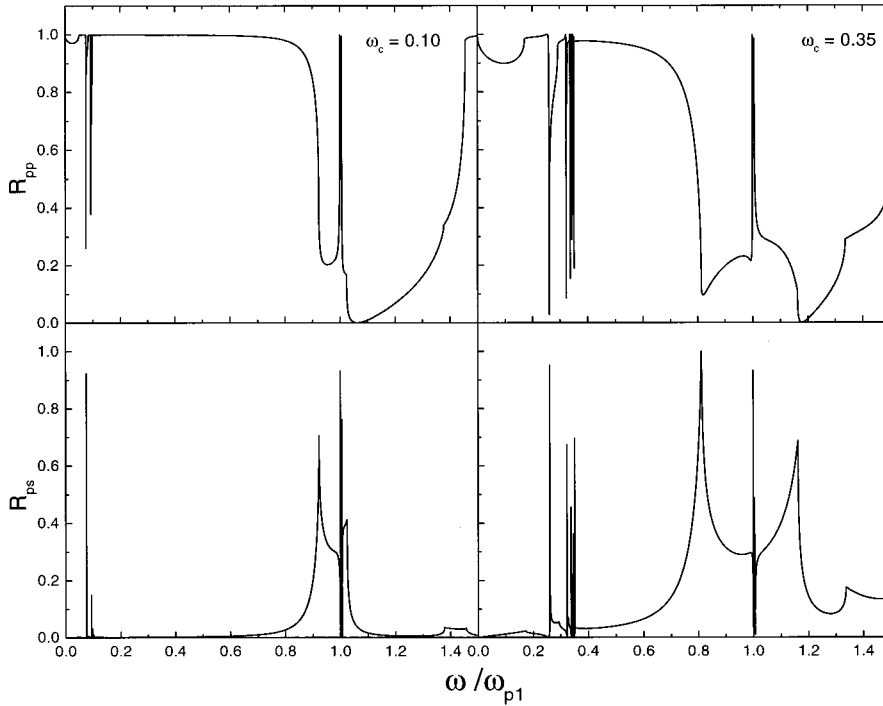


FIG. 4. Reflectivities R_{pp} in the upper panels and R_{ps} in the lower panels for superlattices of alternating a semiconductor layer and an isotropic insulator, as functions of the applied magnetic field for the parameters of Fig. 2. For simplicity, vacuum is taken as the insulator.

over, when the real parts of p_i vanish, no mode propagates and the reflectivity ($R_{pp}^2 + R_{ps}^2 = R^2$) goes to unit. In this case, finite imaginary parts of p_i , $i=1,2$ take place, yielding exponentially evanescent modes away from the surface into the bulk. When p_1 is real and p_2 is imaginary or vice versa, we will obtain a pseudosurface mode of the truncated superlattice. In Fig. 4 we exhibit the behavior of R_{pp} in the upper panel and R_{ps} in the lower panel for a truncated stratified medium, for the same parameters of Fig. 2. The reflectivity displays Fabry-Perot resonances as well as minibands and minigaps of bulk mode propagation in the superlattice and a shift to lower frequencies as ω_c decreases.

We now describe results of the binary semiconductor superlattices. In Fig. 5 we display the dispersion relations ω vs $p_i d$, with $i=1,2$, of the collective normal modes of magne-

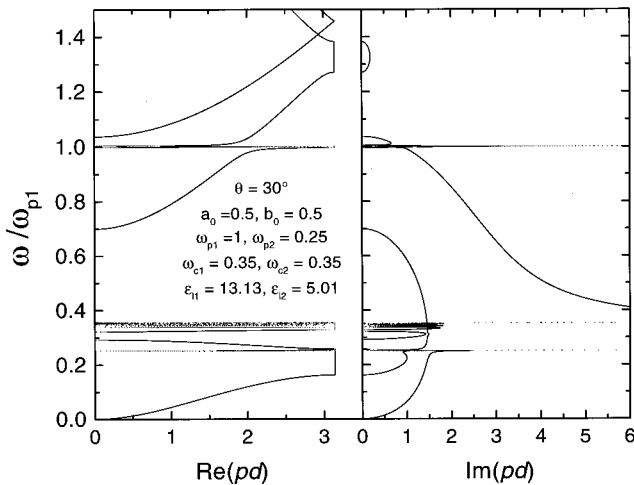


FIG. 5. Collective normal-mode dispersion relations of the binary semiconductor superlattices. Left panel is for the real part and right panel for the imaginary part of Bloch's wave vector. Parameters are shown in the figure.

toplasma systems for the structural parameters $a_0 = b_0 = 0.5c/\omega_{p1}$ and cyclotron frequencies $\omega_{c1} = \omega_{c2} = \omega_c = 0.35\omega_{p1}$. Furthermore, we have $\omega_{p2} < \omega_c < \omega_{p1}$. The reduced scheme in the first Brillouin zone is used in the figure. For each wave, we gave the value $Q = (\omega/c)\sin 30^\circ$ to the parallel wave vector. The figure exhibits two wave vectors and contains a rich structure in the vicinities of the plasma and cyclotron frequencies that can be understood in terms of the dispersion relations ω versus α_i ($i=1,2$) of the transverse modes in the infinite crystals. These dispersion relations are shown in Fig. 3. On the other hand, these magnetoplasmon exhibit minibands of wave propagation into the superlattice and minigaps of forbidden bulk waves.

We describe the results of the composed system in terms of the modes of the isolated crystals, as displayed in Fig. 3. At frequencies $\omega < \omega_{p2}$, there exists one bulk wave and one localized mode in medium a and one or two transverse bulk modes in medium b , then this is a pseudosurface mode region (PS₁). Consequently, the structure of the collective excitations is composed of resonances of those propagating modes and their coupling among themselves, with the evanescent fields of the localized waves. Near ω_{p2} , bulk modes have short wavelengths; furthermore, they repeatedly meet the Fabry-Perot resonance condition, yielding the dips in the spectra. For $\omega_{p2} < \omega < \omega_c$, layer a supports exponentially evanescent waves, while layer b has two propagating modes, this induces a surface polariton window (SP₁). Furthermore, all the structures are originated by resonances in layer b , treating these modes as guided waves since they cannot leak out of the layer. However, these modes couple to those of the adjacent layers through the evanescent fields of layer a , causing collective-mode propagation in the superlattice. In $\omega_c < \omega < 0.48 \omega_{p1}$, medium a exhibits a forbidden gap for bulk polaritons and b supports pseudosurface modes, then we obtain a pseudosurface mode (PS₂) region.

Above $0.48 \omega_{p1}$, medium b allows for bulk polaritons,

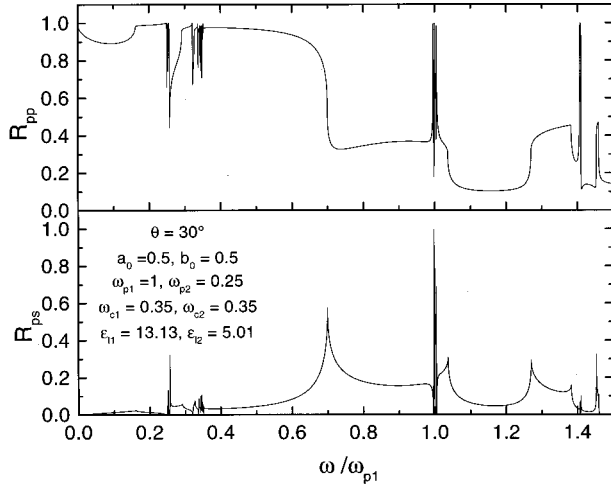


FIG. 6. Reflectivities R_{pp} in the upper panel and R_{ps} in the lower panel, for binary semiconductor superlattices. Parameters are shown in the figure.

but in a , different situations take place. As the frequency increases ($0.48 \omega_{p1} < \omega < 0.84 \omega_{p1}$), medium a allows for surface polaritons, thus we obtain a surface mode region (SP₂). At frequencies $0.84 \omega_{p1} < \omega < \omega_{p1}$, a accounts for one propagating mode, thus we obtain a pseudosurface mode region (PS₃). Finally, at $\omega_{p1} < \omega$, in a exists one bulk polariton and one surface mode, but this surface wave evolves in such a way that eventually it transforms into a bulk polariton. Therefore, we start with a pseudosurface mode region (PS₄) and switch into a bulk polariton (BP) region as ω increases. In summary, coupling of transverse modes of adjacent layers may occur via traveling modes or through evanescent fields, yielding most of the structure in the collective normal mode.

The description presented above on the dispersion relations of the collective normal mode in the superlattice remains qualitatively correct for other choices of cyclotron frequencies, that is, different magnitudes of the applied magnetic field \mathbf{B}_0 . As the magnitude of the field decreases, ω_c decreases, and the resonances below the cyclotron frequency shift to lower energies, allowing for a wider forbidden gap, as the real parts of p_i vanish, while the imaginary parts take finite values.

In Fig. 6 we exhibit in the upper panel the optical reflectance R_{pp} and in the lower panel the conversion from p to s polarization R_{ps} calculated for a semi-infinite superlattice upon which p -polarized light is incident at an angle $\theta = 30^\circ$, for the same parameters of Fig. 5. The feature displayed by R_{pp} and R_{ps} are in close correspondence to that shown by the dispersion relation of the normal mode: there are series of peaks in the vicinity of the plasma and the cyclotron frequencies. All of them are consequences of the Fabry-Perot resonances of the transverse mode in the layers. It is shown that in the forbidden gaps of bulk waves, R_{pp} approaches to unit but is somewhat less due to the finite value of R_{ps} .

It has been pointed out that most of the structure of the dispersion relation of the normal mode is manifested in the vicinity of plasma and cyclotron frequencies, then it is interesting to show how these features are in a close view. For this, in Fig. 7 we depict, in the left panel, the real parts and, in the right panel, the imaginary parts of p_1 and p_2 in the reduced scheme, within the first Brillouin zone below but

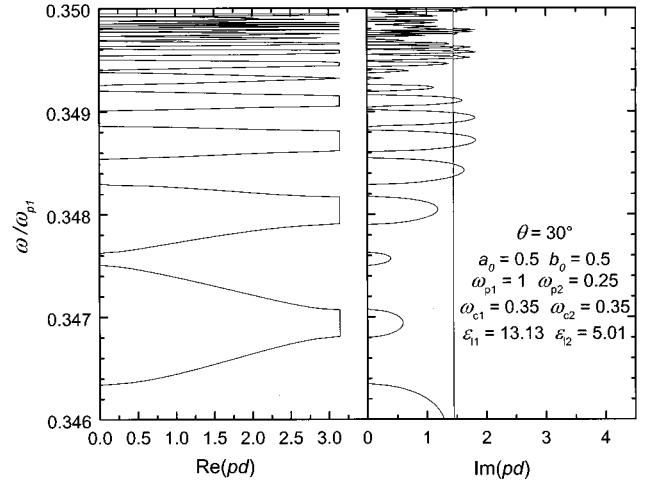


FIG. 7. Collective normal-mode dispersion relations of the binary semiconductor superlattices, in the vicinity of the cyclotron frequency. Left panel shows the real parts and right panel the imaginary parts of Bloch's wave vectors p_1 and p_2 .

near the cyclotron frequency. The figure exhibits allowed or forbidden bands for bulk waves in the superlattice. These are manifested as having finite real or imaginary parts of p_i , respectively. As before, the structure is in close correspondence with the reflectance of light of the semi-infinite system. More precisely, in Fig. 8 R_{pp} is displayed in the upper panel and R_{ps} in the lower panel to exhibit the resonances, allowed and forbidden bands of bulk polaritons. It is also noted that in the forbidden bands $R_{pp} \leq 1$, as produced by finite values of R_{ps} .

In conclusion, we have presented a study of magneto-plasma modes in semiconductor stratified media accounting for an external magnetic \mathbf{B}_0 field in the perpendicular configuration. Incident light with p polarization has been considered to solve the wave equation, construct the 4×4 transfer matrix, then calculate the dispersion relations of the normal mode, the reflectance R_{pp} and the conversion from p - to s -polarization reflection R_{ps} for the binary semiconductor,

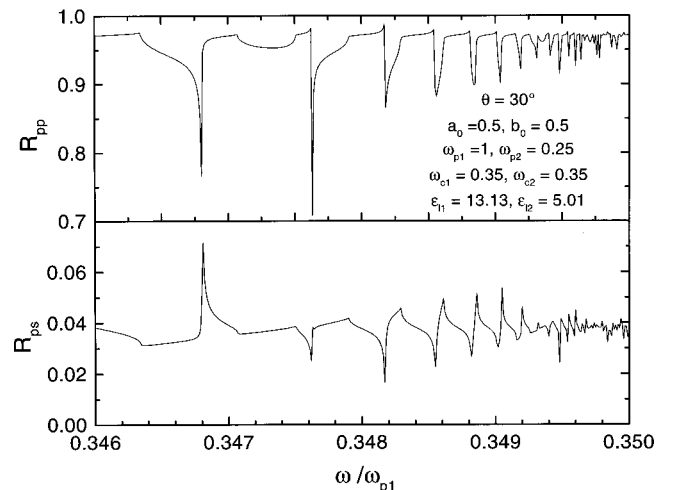


FIG. 8. Reflectivities R_{pp} in the upper panel and R_{ps} in the lower panel, for binary semiconductor superlattices, in the vicinity of the cyclotron frequency. Parameters are as in Fig. 7.

and of a semiconductor alternated with an isotropic insulator superlattice. Results of R_{pp} display structures interpreted in terms of the normal-mode dispersion relations of the collective excitations that either propagate or are localized near the surface of the superlattices, which are originated as the coupling of the modes of adjacent semiconductor layers. Minibands and minigaps of bulk modes in the superlattices are obtained as functions of the structural parameters as well as of the strength of the \mathbf{B}_0 field. As the cyclotron frequency decreases, the Fabry-Perot resonances shift to lower frequen-

cies and at the same time larger forbidden minigaps of bulk modes take place. Variations of the parameters permit us to monitor the minibands for bulk wave propagation, and furthermore allow us to choose frequency regions of bulk modes, useful for applications in filter devices.

ACKNOWLEDGMENT

This work was partially supported by CONACyT–Mexico Grant No. 26363-E.

-
- ¹W. Luis Mochán, M. del Castillo-Mussot, and R. G. Barrera, Phys. Rev. B **35**, 1088 (1987).
²M. del Castillo-Mussot and W. Luis Mochán, Phys. Rev. B **37**, 6763 (1988).
³E. L. Olazagasti, G. H. Coccoletzi, and W. Luis Mochán, Solid State Commun. **78**, 9 (1991).
⁴G. H. Coccoletzi and W. Luis Mochán, Phys. Rev. B **39**, 8403 (1989); G. H. Coccoletzi, A. R. Perucho, and W. Luis Mochán, *ibid.* **44**, 11 514 (1991).
⁵P. Yeh, A. Yariv, and C. S. Hong, J. Opt. Soc. Am. **67**, 423 (1977).

- ⁶P. Halevi and C. Guerra-Vela, Phys. Rev. B **18**, 5248 (1978).
⁷P. Halevi, Phys. Rev. B **23**, 2635 (1981).
⁸M. S. Kushwaha and P. Halevi, Phys. Rev. B **35**, 3879 (1987).
⁹M. S. Kushwaha and P. Halevi, Phys. Rev. B **38**, 12 428 (1988).
¹⁰M. Kushwaha, Phys. Rev. B **40**, 1692 (1989).
¹¹M. Kushwaha, Phys. Rev. B **41**, 5602 (1990).
¹²W. L. Mochán, M. del Castillo-Mussot, and R. A. Vázquez-Nava, Phys. Status Solidi B **174**, 273 (1992); R. A. Vázquez-Nava, M. del Castillo-Mussot, and W. Luis Mochán, Phys. Rev. B **47**, 3971 (1993).